

***Amaranthus cruentus* Flour Edible Films: Influence of Stearic Acid Addition, Plasticizer Concentration, and Emulsion Stirring Speed on Water Vapor Permeability and Mechanical Properties**

ELIANE COLLA,[†] PAULO J. DO AMARAL SOBRAL,[‡] AND
 FLORENCIA CECÍLIA MENEGALLI^{*,†}

Department of Food Engineering, FEA-UNICAMP, P.O. Box 6121, Campinas, SP 13081-970, Brazil,
 and ZEA-FZEA-USP, P.O. Box 23, 13635-900 Pirassununga (SP), Brazil

Films forming solutions composed of Amaranth (*Amaranthus cruentus*) flour (4.0 g/100 mL), stearic acid (5–15 g/100 g of flour), and glycerol (25–35 g/100 g of flour) were prepared by an emulsification process, with varying stirring speed values (6640–13360 rpm). The influence of these parameters (stearic acid and glycerol concentrations and stirring speed) on the water vapor barrier and mechanical properties of films was evaluated using the response surface methodology (RSM). Other characterizations, including microstructure, water solubility, and oxygen permeability, were performed in optimized films. According to statistical analysis results, the optimized conditions corresponded to 10 g of stearic acid/100 g of flour, 26 g of glycerol/100 g of flour, and a stirring speed of 12 000 rpm. The films produced under these conditions exhibited superior mechanical properties (2.5 N puncture force, 2.6 MPa tensile strength, and 148% elongation at break) in comparison to those of other protein and polysaccharide composite films, low solubility (15.2%), and optimal barrier properties (WVP of 8.9×10^{-11} g m⁻¹ s⁻¹ Pa⁻¹ and oxygen permeability of 2.36×10^{-13} cm³ m⁻¹ s⁻¹ Pa⁻¹).

KEYWORDS: Edible films; *Amaranthus cruentus*; lipids; mechanical properties; water vapor permeability

INTRODUCTION

The potential of edible films made from a variety of materials to control water transfer and improve food quality and shelf life has been extensively reviewed in the past decade (1, 2). Polysaccharides and proteins derived from several sources are the mainly studied materials, and the addition of lipid components to improve the water vapor barrier of the films has been the focus of a number of studies (3–5).

The interest in combining polysaccharides, proteins, and lipids is due to the advantages and disadvantages of these components (6). Polysaccharides and proteins have good gas, aroma, and lipid barriers and can also adhere to fruits or vegetable cut surfaces, but they are inefficient against water transfer because of its hydrophilic characteristics. Lipids, on the other hand, offer high water barrier properties; however, they form brittle films causing anaerobic conditions at higher storage temperatures and not sticking to hydrophilic cut surfaces (4, 7).

The use of natural blends of protein, polysaccharides, and lipids directly obtained from agricultural sources takes advantage of each component in the original system and appears to be a new opportunity for material in the area of edible films (8, 9). The *Amaranthus cruentus* flour can be considered such a natural

mixture and consequently an interesting source of raw material for edible film technology (8).

Amaranth (*Amaranthus* spp.) is a tiny grain (~1 mm diameter) typical from South America, one species (*A. cruentus*) of which is composed of 15–22% protein (rich in lysine), 3.0–11.5% fat, and 9–16% dietary fiber, depending on the cultivation technique and environmental effects. The Amaranth main constituent is the starch (48–62%), which has an amylose content of ~10–19% (depending of the variety) and small granule size (<1 μm), characteristics that allow easier dispersion, and hence, it may yield good properties in resultant films (10, 11).

A composite film made of a protein or polysaccharide (or from a mixture of both) and lipids can be divided into laminates (lipid as a distinct layer within or atop the biopolymeric films) and emulsions (lipid uniformly dispersed throughout the film structure) (12). In the case of emulsified films, lipid particle size has a great influence on the water vapor permeability. According to Debeaufort and Voilley (13) and Perez-Gago and Krochta (14), the barrier efficiency increases with the decrease in lipid globule size and with the distribution of homogeneous hydrophobic substances. Therefore, the stirring speed during the emulsification process can be considered as an important factor in obtaining homogeneous films and had a great influence on their performance (15).

The aim of this work was to produce composite films of *A. cruentus* flour and stearic acid, to provide an additional water

* Corresponding author. Telephone: +55-19-37884088. Fax: +55-19-37884027. E-mail: fcm@fea.unicamp.br (F.C.M.) or pjsobral@usp.br (P.J.d.A.S.).

[†] FEA-UNICAMP.

[‡] ZEA-FZEA-USP.

Table 1. Central Composite Design Matrix with Code and Real Values of the Variables and Responses to Water Vapor Permeability (WVP) and Mechanical Properties (PF, TS, and ELO)^a

run	[stearic acid] (x_1) ^b (g/100 g of flour)	[glycerol] (x_2) ^b (g/100 g of flour)	stirring speed (x_3) ^b (rpm)	WVP ($\times 10^{-10}$ g m ⁻¹ s ⁻¹ Pa ⁻¹)	PF (N)	TS (MPa)	ELO (%)
1	7 (-1)	27 (-1)	8000 (-1)	1.97	1.8	2.0	120.1
2	13 (+1)	27 (-1)	8000 (-1)	1.53	1.8	1.7	210.0
3	7 (-1)	33 (+1)	8000 (-1)	2.10	1.2	2.1	269.3
4	13 (+1)	33 (+1)	8000 (-1)	1.80	1.2	0.8	344.3
5	7 (-1)	27 (-1)	12000 (+1)	2.11	2.1	3.0	74.2
6	13 (+1)	27 (-1)	12000 (+1)	1.03	1.9	1.4	280.7
7	7 (-1)	33 (+1)	12000 (+1)	1.53	1.4	1.1	470.7
8	13 (+1)	33 (+1)	12000 (+1)	1.56	1.3	0.9	510.0
9	5 (-1.68)	30 (0)	10000 (0)	1.97	1.7	1.8	502.0
10	15 (+1.68)	30 (0)	10000 (0)	1.25	1.5	1.4	620.0
11	10 (0)	25 (-1.68)	10000 (0)	1.25	2.1	2.3	113.0
12	10 (0)	35 (+1.68)	10000 (0)	1.67	1.1	0.8	420.0
13	10 (0)	30 (0)	6640 (-1.68)	1.44	1.6	1.2	230.0
14	10 (0)	30 (0)	13360 (+1.68)	1.33	2.0	2.0	371.6
15	10 (0)	30 (0)	10000 (0)	1.19	1.7	1.2	284.1
16	10 (0)	30 (0)	10000 (0)	1.17	1.7	1.1	277.2
17	10 (0)	30 (0)	10000 (0)	1.19	1.6	1.2	267.7

^a PF, puncture force; TS, tensile strength; ELO, elongation at break. ^b Independent variable values (the values in parentheses are the coded variable values).

vapor barrier to the films. The stearic acid was used because of its highly regarded characteristics reported in the literature, especially the melting point (67–68 °C), which is compatible with the denaturation temperature of the proteins present in amaranth flour, ~70 °C according to Martínez et al. (16). The response surface methodology was applied for the optimization of stearic acid and plasticizer concentrations and the stirring speed of the suspension in the step of lipid emulsification. Other process parameters (temperature, pH adjustment, and drying conditions) were previously determined (8).

MATERIALS AND METHODS

Film Constituents and Reagents. Mature seeds of Amaranth (*A. cruentus*) cultivar BRS Alegria were provided by Embrapa Cerrados (Brazilian Company of Agropecuary Research, Federal District, Brazil). After being harvested, the seeds were cleaned up and stored at 20 °C in sealed containers until they were tested. Glycerol, stearic acid, NaOH, and HCl were analytical reagent grade and were purchased from Synth (São Paulo, Brazil).

Amaranth Flour Production. The production of amaranth flour was performed according to the methodology described by Perez et al. (17) regarding minor modifications. Amaranth seeds (200 g) were steeped for 24 h in 1.0 L of a 0.25% (w/v) NaOH solution and were further washed with distilled water and milled with enough NaOH solution at 5 °C to avoid heating during milling. The ground slurry was screened through three sieves: 80-, 200-, and 270-mesh. The milling–sieving procedure was repeated four times until there was no more starchlike color in the ground slurry. The suspension containing the amaranth flour was neutralized with 0.2 N HCl to recovery proteins, which are soluble at alkaline pH values (reaching a maximum at pH 10), according to Salcedo-Chávez et al. (18), and centrifuged at 840g for 20 min. The precipitate was resuspended in distilled water and freeze-dried at –52 °C under vacuum for 48 h in a laboratory scale freeze-drier (model FD3, Heto, Allerød, Denmark). The obtained flour was passed through an 80-mesh sieve to standardize the final granulometry and stored at 5 °C in sealed containers until it was used.

Preparation of Films and Conditioning. The amaranth flour concentration (4.0 g/100 mL solution) and pH (10.7, adjusted with 1.0 N NaOH) of the suspension for protein solubilization was previously established, in a preliminary study (8). The studied levels of glycerol (plasticizer) were 25, 27, 30, 33, and 35 g/100 g of flour, and for stearic acid, the concentrations were 5, 7, 10, 13, and 15 g/100 g of flour, defined according to the experimental design that was used (Table 1).

Films were prepared using a solution of amaranth flour and distilled water, which was mixed until the temperature reached 50 °C, when

the pH was adjusted. The heating process was maintained until 80 °C, when glycerol and stearic acid were added. After the lipid had melted, the hot solution was immediately emulsified using an Ultra-Turrax homogenizer (model T18-Basic, IKA Works Brazil, Jacarepaguá, Brazil) for 3 min at speed values defined by the experimental design (6640, 8000, 10 000, 12 000, and 13 360 rpm). The solution was cooled in an ice bath and kept under vacuum for the removal of air bubbles or any dissolved air, for approximately 3 h. Afterward, the filmogenic solution was poured and spread evenly over a Teflon surface (18 cm \times 21 cm). The weight was controlled (± 0.01 g) with a semianalytical balance (AM5500, Marte, São Paulo, Brazil) to obtain a constant thickness. The film-forming solutions were dehydrated in an oven with air renewal and circulation with temperature and relative humidity system controls (model MA 415UR, Marconi, Piracicaba, Brazil) at 40 °C and 55% relative humidity (RH) for 16–18 h, when the equilibrium moisture was reached. Dried films were peeled off the casting surface, cut into adequate samples, and conditioned at 25 °C and 58% RH in desiccators with a saturated solution of NaBr for 72 h prior to characterization. The film thickness was measured using a micrometer (model FOW72-229-001, Fowler, Newcastle, CA) with a range of 0–1 in. and an accuracy of 0.0001 in. The mean thicknesses (micrometers) of the films were determined from the average of 15 measurements made at five different locations.

Experimental Design. A 2³ full-factorial central composite design (star configuration) with 6 axial and 3 central points (triplicate only at the central point), resulting in 17 experiments, was used to obtain a second-order model for prediction of water vapor permeability and mechanical properties (puncture force, tensile strength, and elongation at break) (dependent variable) as a function of three variables (independent variables): stearic acid (x_1) and glycerol (x_2) concentrations and stirring speed (x_3). The statistical design and the coded and real values of these variables are given in Table 1. All experiments were performed randomly, and data were treated with the aid of STATISTICA 5.0 from Statsoft Inc.

Characterization of Amaranth Flour Films. Amaranth flour films were characterized by determinations of water vapor permeability (WVP) and mechanical properties. The films obtained under optimized conditions (stearic acid and glycerol concentrations and stirring speed) were also analyzed by scanning electron microscopy (SEM), and the oxygen permeability and solubility in water were determined.

Water vapor permeability (WVP) tests were conducted using ASTM (19), method E96-95, considering the modifications proposed by Gontard et al. (20). Each film sample was sealed over the circular opening of a permeation cell containing silica gel. These cells were placed on desiccators with distilled water kept at 25 °C. After the samples had reached steady-state conditions (~20 h), the cell weight was measured each 24 h, for 7 days, using a semianalytical balance

(AM5500, Marte). The WVP was calculated as

$$\text{WVP} = \frac{w}{t} \frac{x}{\Delta P} \quad (1)$$

where x is the average thickness of the amaranth flour films, A is the permeation area (0.00091 m^2), ΔP is the difference between the partial pressure of the atmosphere over silica gel and over pure water (3.168 kPa, at 25 °C), and the term w/t was calculated by linear regression using data of weight gain as a function of time. All tests were performed in triplicate.

Mechanical properties were determined by puncture tests (puncture force, PF) and tensile tests (tensile strength, TS, and elongation at break, ELO) using a TA-XT2i Stable Micro Systems texture analyzer (SMS, Surrey, England). In puncture tests, sample films were fixed in a 34 mm diameter cell and perforated by a 3 mm diameter cylindrical probe, moving at 1 mm/s (20, 21). Tensile strength and elongation at break measurements were acquired following the procedure outlined in ASTM method D882-97 (22). Sample films were cut into 2.54 cm wide strips at least 10 cm in length. The initial grip separation was set at 80 mm and the crosshead speed at 1.0 mm/s. The PF (newtons), TS (megapascals), and ELO (percent) were calculated using Texture Expert version 1.15 (SMS). At least five samples from each film were evaluated.

Oxygen permeability measurements were performed on a Mocon Ox-Tran 2/20 instrument equipped with a Coulox sensor (Modern Control, Inc., Minneapolis, MN) operating according to ASTM standard method D3985-81 (23) at atmospheric pressure and room temperature (25 °C). The test cell was composed of two chambers separated by the films (5 cm^2), one of them containing 100% oxygen and the other one containing nitrogen, which induced the transfer of oxygen through the film to the coulometric sensor. The measurements were taken at 25 °C, when oxygen flux had already stabilized, indicating that steady state was reached. The oxygen permeability (OP) was calculated by dividing the oxygen transmission rate by the oxygen pressure and multiplying this result by the mean thickness of the sample.

Solubility in Water. The solubility was calculated as the percentage of dry matter of the film solubilized after immersion for 24 h in water at 25 °C (20). Discs of film (2 cm diameter) were cut, weighed, immersed in 50 mL of distilled water, and slowly and periodically agitated. The amount of dry matter of initial and final samples was determined by drying the samples at 105 °C for 24 h.

SEM analyses were performed using a Leica (Cambridge, England) model LEO440i scanning electron microscope operating at 15 kV. Film samples were maintained in a desiccator with silica gel for 7 days and then gently and randomly broken to investigate the cross section of the samples. A cylindrical aluminum stub cut like a straight chair, upon which the film was fixed using a double-sided copper tape, was used in a specific way to permit the observation of the morphology of the cross section and the surfaces. Further, the stubs with films were coated with gold in a VG Microtech (Cambridge, England) model SC7620 sputter coater for 180 s at 4 mA.

RESULTS AND DISCUSSION

The films obtained from amaranth flour and stearic acid presented moderate opacity (yellowish color) with homogeneous and smooth surfaces, and their thickness was in the range of 85–100 μm . According to the 2^3 central composite design, the results of film characterization are presented in **Table 1**.

Water Vapor Permeability. The lowest value of WVP, among the results obtained for all formulations, was $1.03 \times 10^{-10} \text{ g m}^{-1} \text{ s}^{-1} \text{ Pa}^{-1}$ (**Table 1**), referent to the film containing 13% stearic acid and 27% glycerol, at a stirring speed of 12 000 rpm (run 6). The highest WVP value ($2.11 \times 10^{-10} \text{ g m}^{-1} \text{ s}^{-1} \text{ Pa}^{-1}$) was observed for the formulation obtained at the same stirring speed values and glycerol concentration; however, the stearic acid concentration was 7% (run 5), suggesting an important effect of this fatty acid on the WVP.

The WVP values obtained in this work were lower than those observed by other researches which worked with other biopolymers. Yang and Paulson (24) reported values of $3.61 \times 10^{-10} \text{ g m}^{-1} \text{ s}^{-1} \text{ Pa}^{-1}$ for edible gellan films, emulsified with a 20% stearic/palmitic acid blend, while Anker et al. (12) observed water vapor permeabilities of $\sim 1.81 \times 10^{-9} \text{ g m}^{-1} \text{ s}^{-1} \text{ Pa}^{-1}$ for whey protein isolate films with 11% acetylated monoglyceride. For the films produced with corn starch emulsified with 2.0 g/L of sunflower oil, García et al. (15) indicated permeability values of $\sim 1.94 \times 10^{-10} \text{ g m}^{-1} \text{ s}^{-1} \text{ Pa}^{-1}$.

The low values for WVP can be explained not only by the amaranth flour composition but also by the use of stearic acid. Considering that the amaranth flour used in this study exhibited a natural fat content of $\sim 10\%$ and that these native lipids are naturally structured to the protein chains (25), this condition could perform one of the factors that improve the water vapor barrier of resultant films. Other important values determined for amaranth flour composition were, on a dry basis, $\sim 15\%$ protein and $\sim 11\%$ amylose. Taking into account the use of stearic acid, among the carboxylic acids, many authors reported that stearic acid ($\text{C}_{18}\text{H}_{36}\text{O}_2$), followed by palmitic acid ($\text{C}_{16}\text{H}_{32}\text{O}_2$), exhibited the lowest water vapor permeability, which increases according to the carbon number, since the nonpolar part of the molecule becomes larger (24).

Statistical Analysis and Model Fitting to WVP. The effect estimated for each variable, as well as the interactions between them, was determined with the aid of STATISTICA version 5.0, and the results are listed in **Table 2**. A regression analysis was performed to obtain a second-order model equation (eq 2) for WVP as a function of stearic acid and glycerol concentrations and stirring speed. The statistical significance of this model was checked with an F test (ANOVA), and the results are given in

Table 2. Main Effects and Interaction Analysis for the Response of Water Vapor Permeability and Mechanical Properties of Puncture Force, Tensile Strength, and Elongation at Break

factor	WVP ^a			puncture force			tensile strength			elongation at break		
	effect ($\times 10^{-10} \text{ g m}^{-1} \text{ s}^{-1} \text{ Pa}^{-1}$)	standard error	p value	effect (N)	standard error	p value	effect (MPa)	standard error	p value	effect (%)	standard error	p value
[stearic acid] (x_1)	-0.44	0.008	0.0003 ^b	-0.14	0.022	0.0242 ^b	-0.60	0.039	0.0042 ^b	89.21	4.470	0.0025 ^b
[glycerol] (x_2)	0.15	0.008	0.0030 ^b	-0.62	0.022	0.0012 ^b	-0.83	0.039	0.0022 ^b	208.77	4.470	0.0005 ^b
stirring speed (x_3)	-0.20	0.008	0.0020 ^b	0.20	0.022	0.0111 ^b	0.16	0.039	0.0541	92.29	4.470	0.0023 ^b
x_1x_2	0.32	0.011	0.0011 ^b	0.01	0.028	0.8724	0.12	0.050	0.1451	-45.52	5.840	0.0160 ^b
x_1x	-0.08	0.011	0.0157 ^b	-0.10	0.028	0.0727	-0.04	0.050	0.5566	20.21	5.840	0.0743
x_2x_3	-0.11	0.011	0.0089 ^b	-0.05	0.028	0.2279	-0.41	0.050	0.0151 ^b	85.55	5.840	0.0046 ^b

^a Water vapor permeability. ^b Significant factors ($p < 0.05$ or 95% confidence interval).

Table 3. Analysis of Variance (ANOVA) for the Quadratic Model Description of WVP and Mechanical Properties

source of variation	WVP				puncture force				tensile strength				elongation at break				
	Ss ^a	Df ^b	Ms ^c	F ratio ^d	Ss ^a	Df ^b	Ms ^c	F ratio ^d	Ss ^a	Df ^b	Ms ^c	F ratio ^d	Ss ^a	Df ^b	Ms ^c	F ratio ^d	
regression	1.60	7	0.229	5.87	1.53	4	0.38	54.28	4.42	6	0.74	5.30	331560	8	41445	9.70	
residual	0.35	9	0.039		0.09	12	0.007		1.37	10	0.14		36684	8	4285.5		
lack of fit	0.34	7	0.048		0.08	10	0.008		1.36	8	0.17		36547	6	6092.2		
pure error	0.005	2	0.003		0.003	2	0.002		0.01	2	0.005		136	2	68.22		
total	1.95	16			1.61	16			5.80	16			368244	16			
		$R^2 = 0.83$ $F_{0.95;7;9} = 3.29$				$R^2 = 0.95$ $F_{0.95;4;12} = 3.26$				$R^2 = 0.76$ $F_{0.95;6;10} = 3.22$				$R^2 = 0.90$ $F_{0.95;8;8} = 3.29$			

^a Sum of squares. ^b Degrees of freedom. ^c Mean square. ^d F ratio is the model significance (regression/residual).

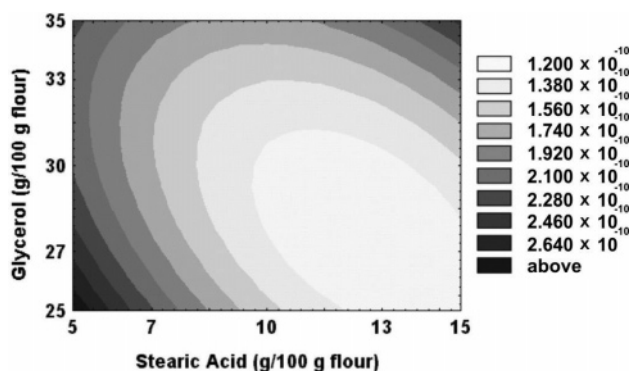


Figure 1. Contour diagram for WVP (grams per meter per second per pascal) as a function of stearic acid and glycerol concentrations (g/100 g of flour).

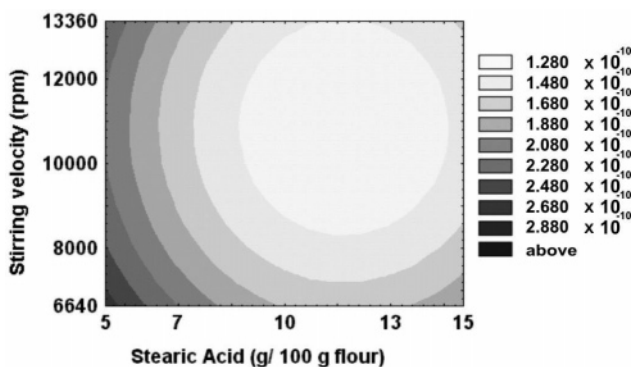


Figure 2. Contour diagram for WVP (grams per meter per second per pascal) as a function of stearic acid concentration (g/100 g of flour) and stirring speed (revolutions per minute).

Table 3. The pure error found was very low, indicating a good reproducibility of the experimental data. According to the *F* test, this model is predictive, since the calculated *F* ratio value (5.87) for the regression related to the residuals is higher than the critical value (3.29) and was used to generate contour plot responses (**Figures 1** and **2**) and response surface (**Figure 3**) for WVP.

$$\text{WVP} = 0.42 - 0.08x_1 + 0.03x_2 - 0.04x_3 + 0.07x_1^2 + 0.05x_2^2 + 0.04x_3^2 + 0.06x_1x_2 \quad (2)$$

where x_1 is the stearic acid concentration, x_2 is the glycerol concentration, and x_3 is the stirring speed.

It can be seen in **Table 2** that all factors exhibited statistically significant effects at the 95% confidence level. The most relevant variables, with regard to the WVP, are the stearic acid concentration and the interaction between this variable and glycerol concentration, since the effects of these factors on WVP

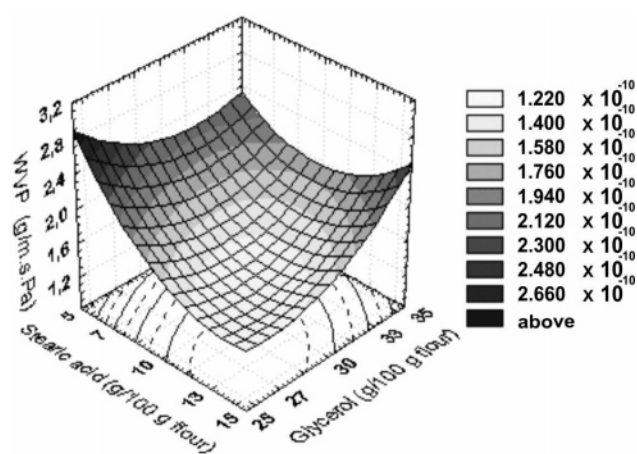


Figure 3. Response surface for WVP (grams per meter per second per pascal) as a function of stearic acid and glycerol concentrations (g/100 g of flour).

were greater than the others. Stearic acid showed a negative effect on WVP, due to its hydrophobicity; consequently, a decrease in WVP values was observed with the increase in stearic acid concentration, which can be confirmed by contour plot responses shown in **Figures 1** and **2**. However, by the response surface (**Figure 3**) analysis, it was possible to verify that this effect tends to change with the increase in glycerol content, confirming that the interaction between stearic acid and glycerol concentrations plays an important role in the WVP of the films obtained in this work. When the glycerol concentration was fixed at 25 g/100 g of flour, the values of WVP decreased continuously with the increase in the amount of stearic acid added; however, at high levels of glycerol (35 g/100 g of flour), WVP was enhanced at stearic acid concentrations of >12%. Sapru and Labuza (26) explained that the increase in the permeability for lipid concentrations higher than a critical value is due to the formation of large fat crystals, allowing interstitial zones free of lipids, which favor moisture migrations.

As expected, the glycerol concentration had a positive effect on WVP (**Table 2** and **Figure 1**), since this plasticizer is hygroscopic and increases the mobility of the molecules through the film structure (20), and it is possible that this increase in molecular mobility caused crystallization of the fatty acid.

As for the stearic acid concentration, the stirring speed had a negative effect on WVP (**Table 2**). According to Péroval et al. (4), the particle size of added lipids in the final film structure is an important factor for WVP; the authors have also reported that the decrease in lipid particle size correlates well with the reduction of WVP, which can be explained by the presence of a large number of spherical particles uniformly dispersed in the film matrix.

On the basis of these observations and statistical analysis results, the best water vapor permeability was $\sim 1.2 \times 10^{-10} \text{ g m}^{-1} \text{ s}^{-1} \text{ Pa}^{-1}$ for the optimum conditions defined as follows: 11.5% stearic acid, 28.5% glycerol, and 11 000 rpm stirring speed.

Mechanical Properties. Under conditions of stress that would occur during processing, such as handling and storage, the expected film integrity can be indicated by its mechanical properties. The resistance and flexibility of films can be described by its tensile strength (TS), puncture force (PF), and elongation at break (ELO) (27). These results are listed in **Table 1**. As can be seen, the film elaborated according to run 5, with 7% stearic acid and 27% glycerol at a stirring speed of 12 000 rpm, showed the highest PF (2.1 N) and TS (3.0 MPa). However, under these conditions, the lowest ELO (74.2%) was observed, whereas the higher ELO (620%) was detected for the films produced with the highest concentration of stearic acid (15%) (run 10 in **Table 1**). This behavior can be more effectively explained by the analysis of the effects of the variables studied over these properties, obtained by the statistical analysis given in **Table 2**. Both the stearic acid concentration and the glycerol concentration had negative effects on puncture force and tensile strength but a positive effect on elongation at break. This behavior observed for stearic acid is in agreement with other works and can be explained by a plasticizing effect of this low-molecular weight component (4, 28, 29). According to Péroval et al. (4), the lipids are unable to form a cohesive and continuous matrix. Therefore, the attainment of suitable mechanical properties is directly related to the protein matrix, polysaccharide, or the mixture of both and also the way the lipids are incorporated into this matrix.

The positive effect of stearic acid on elongation at break can probably be explained by its plasticizing effect on the film structure. Pommet et al. (30) studied the wheat gluten plasticization with fatty acids and observed that their plasticizing abilities were intermediate between water and glycerol, in the tested molar range.

According to Sobral et al. (21) and Vanin et al. (31), plasticizers such as glycerol weaken intermolecular forces between the adjacent polymer chains, reducing the glass transition temperature (T_g) of the material. As a consequence, film flexibility and extensibility increase at the same time the material resistance decreases. In this way, the films obtained in this work exhibited reductions in puncture force and tensile strength with major levels of glycerol addition; on the other hand, the films acquired more flexibility under this condition, presenting more elongation before the breaking.

Stirring speed had a positive effect on the mechanical properties (**Table 2**), probably due to the better distribution of the film components in the polymeric matrix, especially the stearic acid distribution, avoiding the formation of pores and regions where fatty acid can accumulate.

Models Fitting to Mechanical Properties. As for the WVP, a regression analysis was performed to obtain second-order model equations (eqs 3–5) for mechanical properties as a function of stearic acid and glycerol concentrations and stirring speed.

$$\text{PF} = 1.66 - 0.07x_1 - 0.31x_2 + 0.10x_3 - 0.05x_2^2 \quad (3)$$

$$\text{TS} = 1.16 - 0.30x_1 - 0.42x_2 + 0.16x_1^2 + 0.13x_2^2 + 0.16x_3^2 - 0.20x_2x_3 \quad (4)$$

$$\text{ELO} = 282.59 + 44.60x_1 + 104.38x_2 + 46.15x_3 + 79.06x_1^2 - 25.06x_2^2 - 12.93x_3^2 - 22.76x_1x_2 + 42.78x_2x_3 \quad (5)$$

where x_1 is the stearic acid concentration, x_2 is the glycerol concentration, and x_3 is the stirring speed.

The results of the F test (ANOVA) used to verify the statistical significance of these models are listed in **Table 3**. According to the F test, these models are predictive, since the calculated F ratio for the regression related to the residuals is higher than the critical value for puncture force and tensile strength, and elongation at break.

The coded models (eqs 3–5) were used to generate contour plot responses for the mechanical properties (**Figures 4–8**). The negative effects of the glycerol and stearic acid concentration on the puncture force and tensile strength could be confirmed through the contour plot responses represented by **Figures 4 and 6**, since there was a trend of the increase in these properties as both component levels decrease. The glycerol addition effect was greater than the stearic acid effect, results of which are confirmed in **Table 2**. Statistically similar data were obtained for puncture force in the range of 5–12 g of stearic acid/100 g of flour (**Figure 4**), while for the glycerol, this range was more reduced, with concentrations between 25 and 28 g/100 g of flour (**Figure 4**). The effects of stirring speed combined with the stearic acid effect are listed in **Figure 5**.

Stirring speed was not a significant factor (at a 95% confidence level) over tensile strength (**Figure 7**), since the use of any condition in the range studied resulted in statistically similar values for tensile strength.

The plasticizer effect of the stearic acid addition is shown in **Figure 8**, since it was possible to verify that when the level

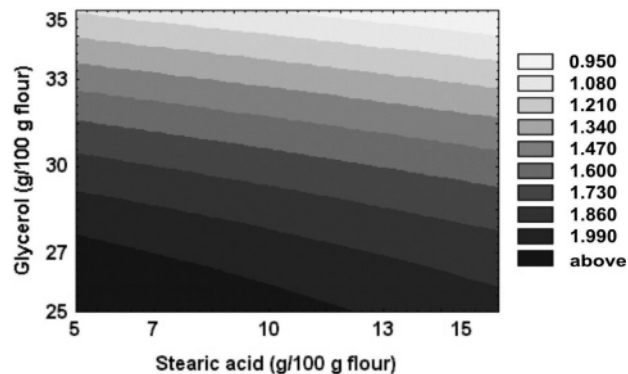


Figure 4. Contour diagram for puncture force (newtons) as a function of stearic acid and glycerol concentrations (g/100 g of flour).

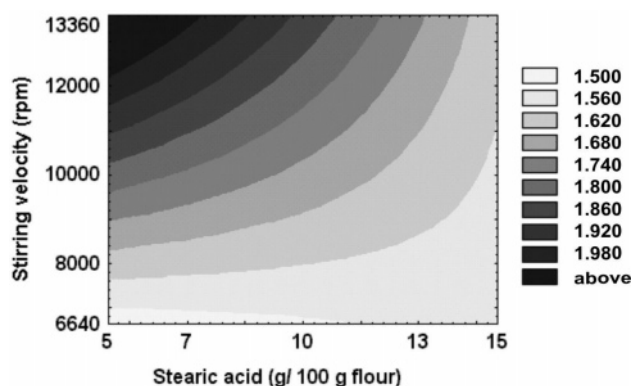


Figure 5. Contour diagram for puncture force (newtons) as a function of stearic acid concentration (g/100 g of flour) and stirring speed (revolutions per minute).

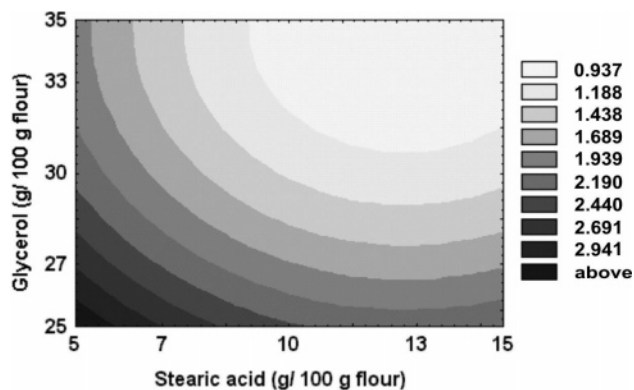


Figure 6. Contour diagram for tensile strength (megapascals) as a function of stearic acid and glycerol concentrations (g/100 g of flour).

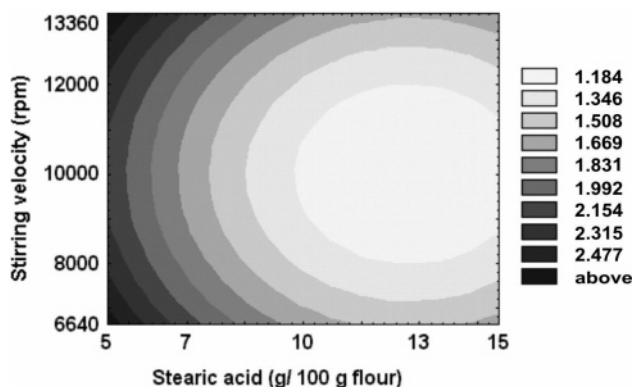


Figure 7. Contour diagram for tensile strength (megapascals) as a function of stirring speed (revolutions per minute) and stearic acid concentration (g/100 g of flour).

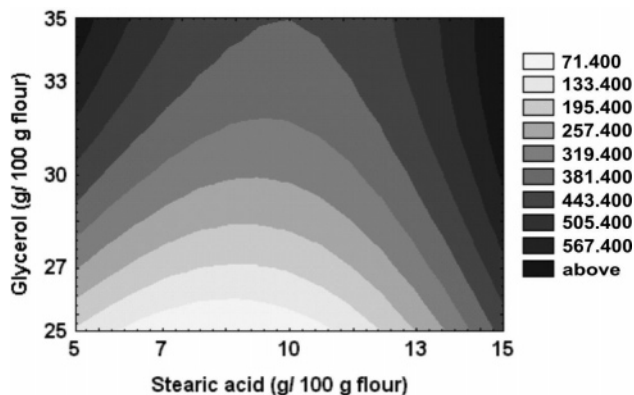


Figure 8. Contour diagram for elongation at break (percent) as a function of stearic acid and glycerol concentrations (g/100 g of flour).

addition of stearic acid was fixed in 15 g/100 g of flour (major level of addition), statistically similar results for elongation were obtained with the increase in glycerol concentration. In other words, the presence of glycerol is less important to the film's flexibility when sufficient stearic acid is added to provide a plasticizer effect to the film structure. On the other hand, the importance of glycerol could be confirmed when stearic acid is fixed at the lowest level that was studied (5 g/100 g of flour). Under this condition, the increase in the glycerol concentration is very important for providing more elongation to films, since in the range of 33–35 g of glycerol/100 g of flour, the greatest elongation was observed.

Definition and Characterization of an Optimized Formulation. After analyzing individually the responses obtained for

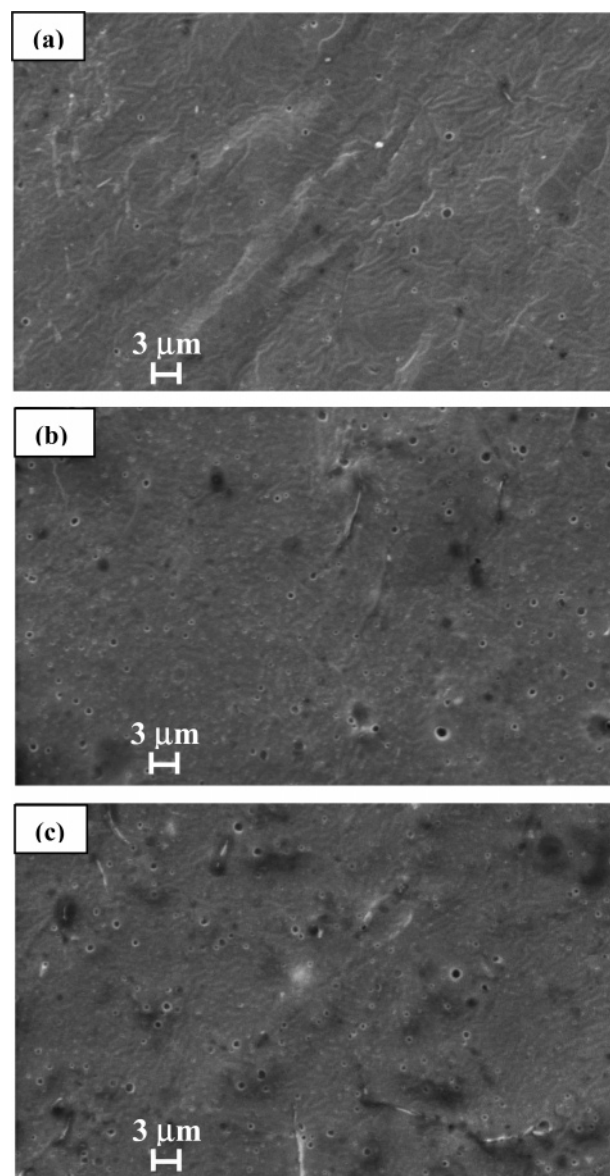


Figure 9. SEM micrographs of amaranth flour films surfaces formulated with (a) 10% stearic acid and 26% glycerol, stirred at 12 000 rpm (optimized conditions); (b) optimized conditions for stearic acid and glycerol concentrations, stirred at 8000 rpm; and (c) optimized conditions for stearic acid and glycerol concentrations, stirred at 6000 rpm.

water vapor permeability and mechanical properties, we defined an optimized formulation to obtain a formulation that is able to provide acceptable mechanical resistance, good flexibility, and, especially, low water vapor permeability, since the main objective of addition of stearic acid to the amaranth flour films was to increase the water vapor barrier. By the analysis of contour plot responses for each property studied, the following optimized conditions were defined: stearic acid concentration of 10 g/100 g of flour, glycerol concentration of 26 g/100 g of flour, and stirring speed of 12 000 rpm.

Amaranth flour films were elaborated according to these optimized conditions. Film microstructural analysis and physical characterizations results are given in **Figures 9** and **10** and in **Table 4**, respectively. Microstructural analysis were also carried out for films prepared at stirring speeds of 6000 and 8000 rpm, to confirm the effect of this parameter on the film structure and to compare with the 12 000 rpm stirring.

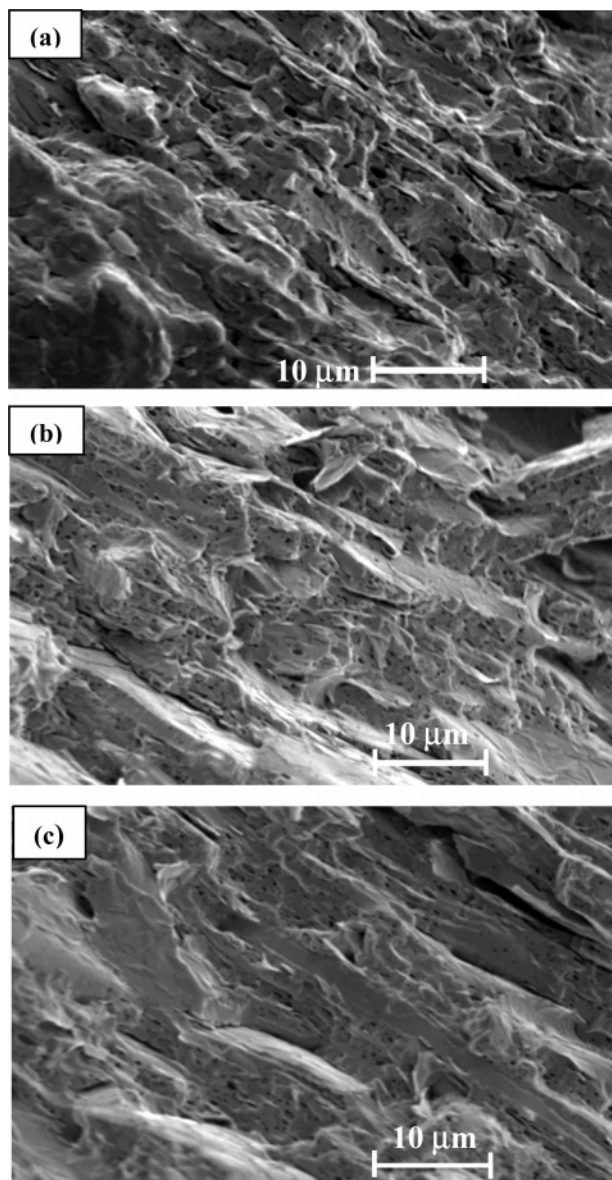


Figure 10. SEM micrographs of a cross section of amaranth flour films (raise of 2500) formulated with (a) 10% stearic acid and 26% glycerol, stirred at 12 000 rpm (optimized conditions); (b) optimized conditions for stearic acid and glycerol concentrations, stirred at 8000 rpm; and (c) optimized conditions for stearic acid and glycerol concentrations, stirred at 6000 rpm.

The surface of the film based on the optimized formulation was homogeneous and regular (**Figure 9a**), suggesting that the emulsification was very efficient, contrary to the results observed by Martin-Polo et al. (32) that described a clearly irregular surface of films based on methyl cellulose and paraffin wax not well incorporated into the bulk of films. It can also be observed in **Figure 9** that film surfaces presented a considerable amount of microporous, probably due to the presence of air bubbles formed during the emulsification process, and that the surfaces were not affected by the emulsifying speed. Monterrey-

Quintero and Sobral (33) also observed microporous in the structure of films based on fish myofibrillar proteins and explained that by the phase-separated glycerol loss during the vacuum preparation of films.

On the other hand, the micrographs of fractured surfaces (**Figure 10**) revealed that the stirring speed affects the internal microstructure of films, which are formed by a spongy structure, probably composed by an emulsified phase of lipids and proteins, cemented by another most dense structure, probably formed from a starch rich non-emulsified phase. Also, it is clear that the increase in the emulsifying speed resulted in a better distribution of both phases. Because of this, these phases are more visible in the condition where a lower speed was used (**Figure 10c**). The better distribution of the lipids with the increase in emulsion stirring speed was also observed by McHugh and Krochta (34), working with whey protein/beeswax emulsion films. This could explain the effect observed of the stirring speed on WVP of the films studied in this work (with an increase in stirring speed we observed a decrease in WVP). According to Martin-Polo et al. (32), an increase in the uniformity of film microstructure implies a decrease in WVP.

The low solubility (15.2%) obtained for the films prepared according to the optimized conditions (**Table 4**) was probably a consequence of the dense matrix (**Figure 9**) of the denatured proteins present in the amaranth flour, since the temperature used for preparing the filmogenic suspension was 82 °C. According to Martínez et al. (16), the denaturation temperatures of albumin and globulin, two proteins present in amaranth grains, were 64 and 70 °C, respectively. Beyond that, the presence of stearic acid has also contributed to this lower solubility of films, due to its hydrophobicity.

Mechanical properties were in the expected range for the optimized formulation, on the basis of the statistical models obtained for each property, except for the elongation at break. The result obtained (148%) was lower than the maximum elongation obtained in the step of optimization (620%). However, it was considered as a long elongation, since this value is greater in relation to those observed by other authors: 2.5% for whey protein films with 20% beeswax, according to Shellhammer and Krochta (35), and ~6% for arabinoxylan films emulsified with 30% hydrogenated palm oil, observed by Phan The et al. (28).

The values of WVP obtained (**Table 4**) for the optimized formulation ($8.9 \times 10^{-11} \text{ g m}^{-1} \text{ s}^{-1} \text{ Pa}^{-1}$) are still higher than those of synthetic films [e.g., $8.4 \times 10^{-11} \text{ g m}^{-1} \text{ s}^{-1} \text{ Pa}^{-1}$ for cellophane, $3.6 \times 10^{-13} \text{ g m}^{-1} \text{ s}^{-1} \text{ Pa}^{-1}$ for LDPE, and $2.2 \times 10^{-13} \text{ g m}^{-1} \text{ s}^{-1} \text{ Pa}^{-1}$ for PVDC (35)] but lower than those found for similar edible films, such as arabinoxylan-based films ($1.8 \times 10^{-10} \text{ g m}^{-1} \text{ s}^{-1} \text{ Pa}^{-1}$) studied by Péroval et al. (4) and gelatin films ($1.1 \times 10^{-10} \text{ g m}^{-1} \text{ s}^{-1} \text{ Pa}^{-1}$) reported by Sobral et al. (21).

The film produced under the optimized conditions exhibited a lower oxygen permeability ($2.36 \times 10^{-13} \text{ cm}^3 \text{ m}^{-1} \text{ s}^{-1} \text{ Pa}^{-1}$) than LDPE ($2.16 \times 10^{-11} \text{ cm}^3 \text{ m}^{-1} \text{ s}^{-1} \text{ Pa}^{-1}$) and edible films based on corn starch plasticized with glycerol ($4.61 \times 10^{-10} \text{ cm}^3 \text{ m}^{-1} \text{ s}^{-1} \text{ Pa}^{-1}$) (15). This behavior could be a consequence of the dense biopolymeric matrix formed by starch and denatured proteins of the amaranth flour, resulting in a system

Table 4. Characterization of the Composite Film from Amaranth Flour and Stearic Acid-Elaborated According to the Optimized Formulation (10 g of stearic acid/100 g of flour, 26 g of glycerol/100 g of flour, stirring speed of 12 000 rpm)

solubility (%)	WVP ($\text{g m}^{-1} \text{ s}^{-1} \text{ Pa}^{-1}$)	oxygen permeability ($\text{cm}^3 \text{ m}^{-1} \text{ s}^{-1} \text{ Pa}^{-1}$)	PS (N)	TS (MPa)	ELO (%)
15.20	8.9×10^{-11}	2.36×10^{-13}	2.53	2.60	148.0

with a small free volume and, consequently, inhibiting the diffusion process.

The presence of stearic acid (10% under the optimized conditions) is another factor that could have influenced the low oxygen permeability that was obtained, since it decreases the hydrophilic characteristics of the film. Nevertheless, the low oxygen permeability appears to be due to amaranth flour itself, since Tapia-Blácido et al. (8, 9) determined an oxygen permeability value of $2.54 \times 10^{-13} \text{ cm}^3 \text{ m}^{-1} \text{ s}^{-1} \text{ Pa}^{-1}$ for films made from *A. cruentus* flour (without lipid addition), which was similar to the result observed in this work ($2.36 \times 10^{-13} \text{ cm}^3 \text{ m}^{-1} \text{ s}^{-1} \text{ Pa}^{-1}$) and the value of $6.5 \times 10^{-13} \text{ cm}^3 \text{ m}^{-1} \text{ s}^{-1} \text{ Pa}^{-1}$ for films made from *Amaranthus caudatus*.

Ayranci and Tunc (5) studied the effect of addition of stearic acid on the oxygen permeability of films made from methyl cellulose and observed a reduction ($\sim 7\text{--}5.2 \times 10^{-9} \text{ g day}^{-1} \text{ Pa}^{-1} \text{ m}^{-1}$) in the rate of O_2 transmission when an addition of 5% stearic acid was performed. However, increasing the stearic acid content of the film (15 g/100 g of methyl cellulose) enhances the oxygen permeability, and the authors attributed such an increase to the formation of holes in the crystal structure of edible films as the stearic acid content increases.

Conclusions. Our results indicate that *A. cruentus* flour is an interesting source of raw material for edible film production, following the actual trends in the use of natural mixtures of protein, starch, and lipids to reach the desired properties for edible films. Besides that, incorporation of stearic acid into a polymeric matrix provided an additional water vapor barrier to the films. The statistical methodology allowed us to find the optimal conditions for studied variables, which were stearic acid and glycerol concentrations of 10 and 26 g/100 g of flour, respectively, and a stirring speed at 12 000 rpm. The mechanical properties of the films obtained under these conditions were a 2.53 N puncture force, a 2.60 MPa tensile strength, and a 148% elongation at break. The solubility value that was found was around 15%, and barrier properties were $8.9 \times 10^{-11} \text{ g m}^{-1} \text{ s}^{-1} \text{ Pa}^{-1}$ for water vapor permeability and $2.4 \times 10^{-13} \text{ cm}^3 \text{ m}^{-1} \text{ s}^{-1} \text{ Pa}^{-1}$ for oxygen permeability.

ACKNOWLEDGMENT

We thank the Brazilian Company of Agropecuary Research (EMBRAPA) for providing the *A. cruentus* grains.

LITERATURE CITED

- Krochta, J. M.; De-Mulder-Johnston, C. Edible and biodegradable polymer films: Challenges and opportunities. *Food Technol.* **1997**, *51*, 61–74.
- Koelsch, C. Edible water vapor barriers: Properties and promise. *Trends Food Sci. Technol.* **1994**, *5*, 76–81.
- Morillon, V.; Debeaufort, F.; Blond, G.; Capelle, M.; Voilley, A. Factors affecting the moisture permeability of lipid-based edible films: A review. *Crit. Rev. Food Sci.* **2002**, *2*, 67–89.
- Péroval, C.; Debeaufort, F.; Despré, D.; Voilley, A. Edible arabinoxylan-based films. 1. Effects of lipid type on water vapor permeability, film structure, and other physical characteristics. *J. Agric. Food Chem.* **2002**, *50*, 3977–3983.
- Ayranci, E.; Tunc, S. A method for the measurement of the oxygen permeability and the development of edible films to reduce the rate of oxidative reactions in fresh foods. *Food Chem.* **2003**, *80*, 423–431.
- Baldwin, E. A.; Nisperos, M. O.; Baker, R. A. Use of edible coatings to preserve quality of lightly (and slightly) processed products. *Crit. Rev. Food Sci.* **1995**, *35*, 509–524.
- Kester, J. J.; Fennema, O. R. Edible films and coatings: A review. *Food Technol.* **1988**, *42*, 47–59.
- Tapia-Blácido, D.; Sobral, P. J. A.; Menegalli, F. C. Development and characterization of edible films based on amaranth flour (*Amaranthus caudatus*). *J. Food Eng.* **2005**, *67*, 215–223.
- Tapia-Blácido, D.; Sobral, P. J. A.; Menegalli, F. C. Effects of drying temperature and relative humidity on the mechanical properties of amaranth flour films plasticized with glycerol. *Braz. J. Chem. Eng.* **2005**, *22*, 249–256.
- Tosi, E. A.; Ré, E.; Lucero, H.; Masciarelli, R. Dietary fiber obtained from Amaranth (*Amaranthus cruentus*) grain by differential milling. *Food Chem.* **2001**, *73*, 441–443.
- Sugimoto, Y.; Yamada, K.; Sakamoto, S. Some properties of normal and waxy-type starches of *Amaranthus Hypochondriacus*. *Starch/Staerke* **1981**, *33*, 112–116.
- Anker, M.; Berntsen, J.; Hermansson, A.; Stading, M. Improved water vapor barrier of whey protein films by addition of an acetylated monoglyceride. *Innovations Food Sci. Emerging Technol.* **2002**, *3*, 254–260.
- Debeaufort, F.; Voilley, A. Effect of surfactants and drying rate on barrier properties of emulsified films. *Int. J. Food Sci. Technol.* **1995**, *30*, 183–190.
- Perez-Gago, M. B.; Krochta, J. Lipid particle size effect on the water vapor permeability and mechanical properties of whey protein/beeswax emulsion films. *J. Agric. Food Chem.* **2001**, *49*, 996–1002.
- García, M. A.; Martino, M. N.; Zaritzky, N. E. Lipid addition to improve barrier properties of edible starch-based films and coatings. *J. Food Sci.* **2000**, *65*, 941–947.
- Martínez, E. N.; Castellani, O. F.; Añón, C. M. Common molecular features among amaranth storage proteins. *J. Agric. Food Chem.* **1997**, *45*, 3832–3839.
- Perez, E.; Bahnssey, Y. A.; Breene, W. M. A simple laboratory scale method for isolation of amaranth starch. *Starch/Staerke* **1993**, *45*, 211–214.
- Salcedo-Chávez, B.; Osuna-Castro, J. A.; Guevara-Lara, F.; Domínguez-Domínguez, J.; Paredes-López, O. Optimization of the isoelectric precipitation method to obtain protein isolates from Amaranth (*Amaranthus cruentus*) seeds. *J. Agric. Food Chem.* **2002**, *50*, 6515–6520.
- ASTM 1995. Designation E96-95: Standard method for water vapor transmission of materials. In *Annual Book of ASTM Standards*; American Society for Testing and Materials: Philadelphia, 1995; pp 785–792.
- Gontard, N.; Duchez, C.; Cuq, J.; Guilbert, S. Edible composite films of wheat gluten and lipids: Water vapor permeability and other physical properties. *Int. J. Food Sci. Technol.* **1994**, *29*, 39–50.
- Sobral, P. J. A.; Menegalli, F. C.; Hubinger, M. D.; Roques, M. A. Mechanical, water vapor barrier and thermal properties of gelatin based edible films. *Food Hydrocolloids* **2001**, *15*, 423–432.
- ASTM 1997. Designation D 882-97: Standard test method for tensile properties of thin plastic sheeting. In *Annual Book of ASTM Standards*; American Society for Testing and Materials: Philadelphia, 1997; pp 159–197.
- ASTM 1989. Designation D 3985-81: Standard test method for gas transmission rate of plastic film and sheeting. In *Annual Book of ASTM Standards*; American Society for Testing and Materials: Philadelphia, 1989.
- Yang, L.; Paulson, A. T. Effects of lipids on mechanical and moisture barrier properties of edible gellan film. *Food Res. Int.* **2000**, *33*, 571–578.
- Tapia-Blácido, D. Edible films development from *Amaranthus cruentus* and *Amaranthus caudatus*. Unpublished Doctoral Thesis, State University of Campinas, Campinas, Brazil, 2006.
- Sapru, V.; Labuza, T. P. Dispersed phase concentration effects on water vapor permeability in composite methyl cellulose-stearic acid edible films. *J. Food Process. Preserv.* **1994**, *18*, 359–368.

- (27) Park, S. K.; Rhee, C. O.; Bae, D. H.; Hettiarachchy, N. S. Mechanical properties and water-vapor permeability of soy-protein films affected by calcium salts and glucono- δ -lactone. *J. Agric. Food Chem.* **2001**, *49*, 2308–2312.
- (28) Phan The, D.; Debeaufort, F.; Péroval, C.; Despré, D.; Courthaudon, J. L.; Voilley, A. Arabinoxylan-lipid-based edible films and coatings. 3. Influence of drying temperature on film structure and functional properties. *J. Agric. Food Chem.* **2002**, *50*, 2423–2428.
- (29) Perez-Gago, M. B.; Krochta, J. Drying temperature effect on water vapor permeability and mechanical properties of whey protein-lipid emulsion films. *J. Agric. Food Chem.* **2000**, *48*, 2687–2692.
- (30) Pommet, M.; Redl, A.; Morel, M.; Guilbert, S. Study of wheat gluten plasticization with fatty acids. *Polymer* **2003**, *44*, 115–122.
- (31) Vanin, F. M.; Sobral, P. J. A.; Menegalli, F. C.; Carvalho, R. A.; Habitante, A. M. Q. B. Effects of plasticizers and their concentrations on thermal and functional properties of gelatin based films. *Food Hydrocolloids* **2005**, *19*, 899–907.
- (32) Martin-Polo, M.; Mauguin, C.; Voilley, A. Hydrophobic films and their efficiency against moisture transfer. 1. Influence of the film preparation technique. *J. Agric. Food Chem.* **1992**, *40*, 407–412.
- (33) Monterrey-Quintero, E. S.; Sobral, P. J. A. Preparo e caracterização de proteínas miofibrilares de tilápia do nilo (*Oreochromis niloticus*) para elaboração de biofilmes. *Pesqui. Agropecu. Bras.* **2000**, *35* (1), 179–189.
- (34) Habig McHugh, T.; Krochta, J. M. Dispersed phase particle size effects on water vapor permeability of whey protein-beeswax edible emulsions films. *J. Food Process. Preserv.* **1994**, *18*, 173–188.
- (35) Shellhammer, T. H.; Krochta, J. M. Whey protein emulsion film performance as affected by lipid type and amount. *J. Food Sci.* **1997**, *62*, 390–394.

Received for review April 20, 2006. Revised manuscript received June 23, 2006. Accepted June 28, 2006. We are thankful for the MS fellowship (E.C.) of CAPES and the PQI fellowship (P.J.d.A.S. and F.C.M.) of CNPq.

JF0611217